

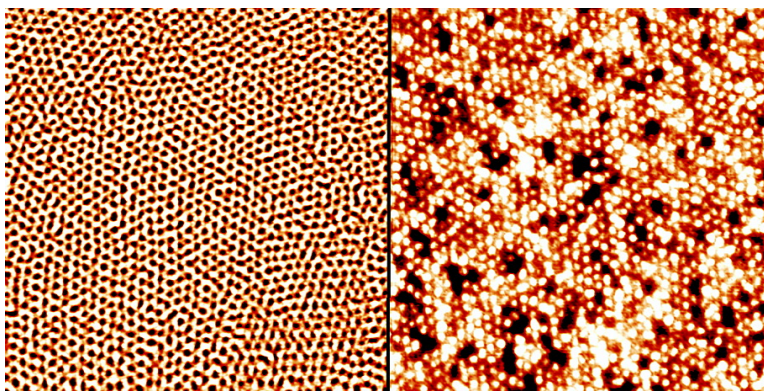
Article

Ordered Reactive Nanomembranes/Nanotemplates from Thin Films of Block Copolymer Supramolecular Assembly

Alexander Sidorenko, Igor Tokarev, Sergiy Minko, and Manfred Stamm

J. Am. Chem. Soc., **2003**, 125 (40), 12211-12216 • DOI: 10.1021/ja036085w • Publication Date (Web): 16 September 2003

Downloaded from <http://pubs.acs.org> on March 29, 2009



More About This Article

Additional resources and features associated with this article are available within the HTML version:

- Supporting Information
- Links to the 33 articles that cite this article, as of the time of this article download
- Access to high resolution figures
- Links to articles and content related to this article
- Copyright permission to reproduce figures and/or text from this article

[View the Full Text HTML](#)



Ordered Reactive Nanomembranes/Nanotemplates from Thin Films of Block Copolymer Supramolecular Assembly

Alexander Sidorenko,[†] Igor Tokarev,[†] Sergiy Minko,^{*,†,‡} and Manfred Stamm[†]

Contribution from the Institut für Polymerforschung Dresden, Hohe Strasse 6, Dresden 01069, Germany, and Department of Chemistry, Clarkson University, Potsdam, New York 13699-5814

Received May 12, 2003; E-mail: sminko@clarkson.edu

Abstract: We report on a unique, very simple method of preparation of reactive membranes and nanotemplates with nanoscopic cylindrical channels on the surface of various inorganic and polymeric substrates. Well-ordered nanostructured thin polymer films have been fabricated from the supramolecular assembly of poly(styrene-*block*-4-vinylpyridine) (PS-PVP) and 2-(4'-hydroxybenzeneazo)benzoic acid (HABA), consisting of cylindrical nanodomains formed by PVP-HABA associates surrounded by PS. Alignment of the domains has been shown to be switched upon exposure to vapors of different solvents from the parallel to perpendicular orientation to the confining surface and vice versa. The alignment of the cylindrical nanodomains is insensitive to the composition of the confining surface due to the self-adaptive behavior of the supramolecular PVP-HABA assembly. Extraction of HABA with selective solvent results in nanomembranes with a hexagonal lattice (24 nm in the period) of hollow channels of 8 nm in the diameter crossing the membrane from the top to the bottom. The walls of the channels are constituted from reactive PVP chains. The channels were filled with Ni clusters via the electrodeposition method to fabricate the ordered array of metallic nanodots of 1.2 tera per cm².

Introduction

Thin films of block copolymers (BC) are the focus of intensive investigations due to their self-assembly into well-ordered periodic structures.¹ BC demonstrate a variety of bulk morphologies (spherical, cylindrical, gyroidal, lamellar) depending on the ratio of block lengths and the segment–segment interaction parameter. The periodicity is determined by the molecular weight of BC and typically is in the range of 10/100 nm.² This class of ordered materials is promising for applications in many fields of nanoscience and technology such as surface patterning, lithography, and templating for the fabrication of information storage devices of terabits per cm² capacity, magnetic and optical materials, nanowires, nanomembranes, etc.^{3,4}

BC thin films confined by copolymer–substrate and copolymer–air (or vacuum) interfaces undergo both surface relaxation and surface reconstruction. It is caused by surface phenomena which induce changes in the periodicity and force one of the blocks to occupy an interface.^{5–9} In the films of practical interest

(thickness in the range of several bulk periods), the surface phenomena dominate over the morphology of the films, hampering the fabrication of the ordered material with the desired orientation of nanoscopic domains. Therefore, in terms of practical applications of the block copolymer thin films, at least three following key problems should be overcome.

First, thin films of BC are to be well ordered to provide the highest density of the domains and an equal distance between them. The widely used approach to improve the order in BC is annealing at temperature above the glass-transition (T_g),¹⁰ resulting in the formation of the thermodynamically stable (or metastable) state and in the improvement of lateral order. Recently, Krausch et al.¹¹ proposed an elegant alternative method to promote self-assembly into nanometer-scale domains. The procedure consists of the controlled swelling of BC thin films in solvent vapor. Solvent quality and swelling ratio may affect the morphology and, particularly, orientation of nanoscopic domains in films of triblock copolymers. Very recently, an approach was suggested by Kramer et al.¹² They explore the phenomenon of topographical confinement (lithographically patterned Si-wafer) to induce a single crystalline order in a single layer of block copolymer spheres.

[†] Institut für Polymerforschung.

[‡] Clarkson University.

(1) Krausch, G.; Magerle, R. *Adv. Mater.* **2002**, *14*, 1579–1583.

(2) Bates, F. S.; Fredrickson, G. H. *Annu. Rev. Phys. Chem.* **1990**, *41*, 525–557.

(3) Minsky, P.; Chaikin, P.; Thomas, E. L. *J. Mater. Sci.* **1995**, *30*, 1987–1992.

(4) Park, M.; Harrison, C.; Chaikin, P. M.; Register, R. A.; Adamson, D. H. *Science* **1997**, *276*, 1401–1404.

(5) Fasolka, M. J.; Mayes, A. M. *Annu. Rev. Mater. Res.* **2001**, *31*, 323–355.

(6) Green, P. F.; Limary, R. *Adv. Colloid Interface Sci.* **2001**, *94*, 53–81.

(7) (a) Peters, R. D.; Yang, X. M.; Wang, Q.; de Pablo, J. J.; Nealey, P. F. *J. Vac. Sci. Technol., B* **2000**, *18*, 3530–3534. (b) Wang, Q.; Nath, S. K.; Graham, M. D.; Nealey, P. F.; de Pablo, J. J. *J. Chem. Phys.* **2001**, *34*, 3458–3470.

(8) Rehse, N.; Knoll, A.; Magerle, R.; Krausch, G. *Macromolecules* **2003**, *36*, 3261–3271.

(9) Huinink, H. P.; van Dijk, M. A.; Brokken-Zijp, J. C. M.; Sevink, G. J. A. *Macromolecules* **2001**, *34*, 5325–5339.

(10) Kim, H.-C.; Russell, T. P. *J. Polym. Sci., Part B: Polym. Phys.* **2001**, *39*, 663–668.

(11) Fukunaga, K.; Elbs, H.; Magerle, R.; Krausch, G. *Macromolecules* **2000**, *33*, 947–953.

(12) Segalman, R. A.; Hexemer, A.; Hayward, R. C.; Kramer E. J. *Macromolecules* **2003**, *36*, 3272–3288.

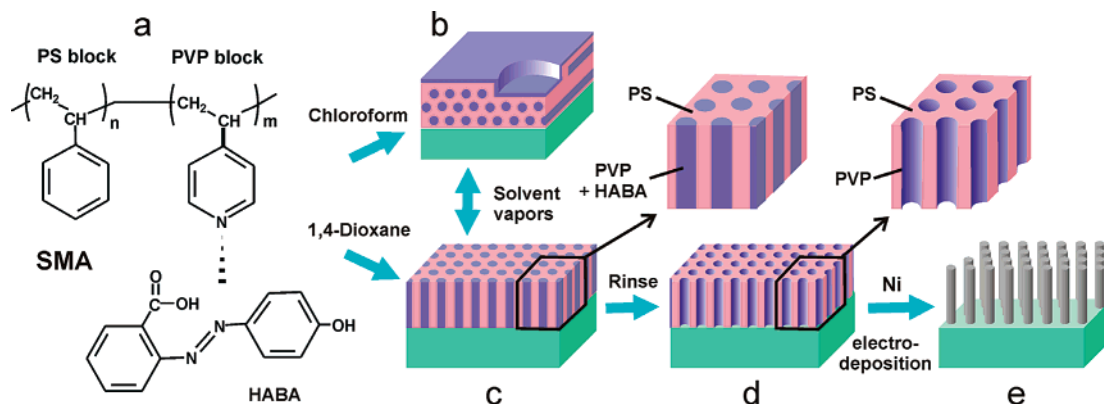


Figure 1. Scheme of the nanotemplate fabrication approach based on the BC assembly.

Second, the desired alignment of the domains (the typical example is represented by cylindrical or lamellar domains oriented perpendicular to the substrate surface) is required for practical application. However, the perpendicular orientation is in contradiction with the tendency of the domains to align parallel to the confining surface caused by the preferential wetting of the interface with one of the blocks.^{2,13} Several approaches have been proposed to overcome this problem. T. P. Russell et al.¹⁴ showed that annealing in an external electric field of a high strength (at least 30 kV/cm) provided the orientation of poly(methyl methacrylate) (PMMA) cylinders or lamellae of a polystyrene-*block*-poly(methyl methacrylate) (PS-PMMA) thin film along the field lines, in either the normal (C \perp) or the in-plane (C \parallel) direction depending on the applied electric field orientation. The effect of external electric field on the BC film structure and on the order–disorder transition temperature was discussed in several publications.^{15,16} Another approach proposed by T. P. Russell et al. consists of the orientation of a BC film by the “neutral surface” of the solid substrate.¹⁷ Also, many recent reports are dedicated to the solvent-induced orientation.^{11,18,19}

Third, most applications require that the minor component forming nanodomains is eliminated to transform the BC film into a membrane/template. T. P. Russell et al.²⁰ proposed UV etching to selectively remove PMMA from the BC film of PS-PMMA. Also, plasma etching was applied for several BC films.⁴ An elegant method based on a polymeric supramolecular assembly was proposed by O. Ikkala et al.²¹ They used hydrogen bonding between 4-vinylpyridine monomer units and 3-pentadecyl phenol (PDP) to modify the morphology of poly(styrene-*block*-4-vinylpyridine) (PS-PVP). The investigation of PS-PVP + PDP in the bulk showed that the supramolecular assembling

of PVP and PDP changed the BC morphology from spherical to cylindrical.²¹ PDP can be easily removed by washing with selective solvent providing nanoscopic channels in the major component matrix.²²

It is a challenging task to develop an appropriate material and technology that is a simple solution to the three above-mentioned problems and allows fast fabrication of well-ordered nanomembranes/nanotemplates from block copolymer films deposited on solid substrate. Here, we report the successful approach based on the idea of adjusting properties of a block copolymer supramolecular assembly with low molar mass additive. This component helps to solve most of the problems: the appropriate alignment, the crystalline-like order, and the easy transformation of the film into a membrane. It is straightforward that the addition of the third component may strongly modify interactions at interfaces and change surface reconstruction. Taking into account the great number of parameters affecting morphology in such a system, our search of the third component was based mainly on a qualitative analysis of hydrogen bonding with BC, a capability to form mesophases, and a capability for the selective extraction from the BC matrix. Finally, we have selected the system from PS-PVP and 2-(4'-hydroxybenzene-azo)benzoic acid (HABA) (Figure 1a). Depending on the experimental conditions, the PS-PVP + HABA supramolecular assembly (SMA) demonstrates microphase separation with hexagonally packed cylinders of either C \perp or C \parallel orientation as shown schematically in Figure 1b,c. Moreover, HABA can be easily removed when it is washed in selective solvent, giving the ordered array of nanochannels (Figure 1d). Finally, electrodeposition throughout the nanotemplate results in the ordered array of metal dots or nanowires (Figure 1e).

Experimental Section

Materials. Poly(styrene-*block*-(4-vinylpyridine)) (PS-PVP), with number average molecular masses (M_n) of PS 35 500 g/mol, PVP 3680 g/mol, $M_w/M_n = 1.06$ for both blocks, was purchased from Polymer Source, Inc. 2-(4'-Hydroxybenzene-azo)benzoic acid (HABA) was purchased from Sigma-Aldrich. The solvents 1,4-dioxane, chloroform, THF, toluene, methanol, and dichloromethane were purchased from Acros Organics and used as is. Silicon wafers {100} and quartz slides were cleaned successively in an ultrasonic bath (dichloromethane) for 15 min and a “piranha” bath (30% H₂O₂, 70% of H₂SO₄, *chemical hazard*) for 40 min at 82 °C, and then thoroughly rinsed with Millipore water and dried under an argon flow.

- (13) Schwark, D.; Vezie, D.; Reffner, J.; Annis, B.; Thomas, E. *J. Mater. Sci. Lett.* **1992**, *11*, 352–355.
 (14) Morkved, T. L.; Lu, M.; Urbas, A. M.; Elrich, E. E.; Jaeger, H. M.; Minsky, P.; Russell, T. P. *Science* **1996**, *273*, 931–933.
 (15) (a) Amundson, K.; Helfand, E.; Patel, S. S.; Quann, X. *Macromolecules* **1991**, *24*, 6546–6548. (b) Amundson, K.; Helfand, E.; Quann, X.; Hudson, S. D.; Smith, S. D. *Macromolecules* **1994**, *27*, 6559–6570.
 (16) Gurovich, E. *Phys. Rev. Lett.* **1995**, *74*, 482–485.
 (17) Huang, E.; Russell, T. P.; Harrison, C.; Chaikin, P. M.; Register, R. A.; Hawker, C. J.; Mays, J. *Macromolecules* **1998**, *31*, 7641–7650.
 (18) (a) Kim, G.; Libera, M. *Macromolecules* **1998**, *31*, 2569–2577. (b) Kim, G.; Libera, M. *Macromolecules* **1998**, *31*, 2670–2672.
 (19) Elbs, H.; Drummer, C.; Abetz, V.; Krausch, G. *Macromolecules* **2002**, *35*, 5570–5577.
 (20) Turn-Albrecht, T.; Steiner, R.; DeRouchey, J.; Stafford, C. M.; Huang, E.; Bal, M.; Tuominen, M.; Hawker, C. J.; Russell, T. P. *Adv. Mater.* **2000**, *12*, 787–791.
 (21) Ruokolainen, J.; Mäkinen, R.; Torkkeli, M.; Mäkelä, T.; Serimaa, R.; ten Birke, G.; Ikkala, O. *Science* **1998**, *280*, 557–560.

- (22) Mäki-Ontto, R.; de Moel, K.; de Odorico, W.; Ruokolainen, J.; Stamm, M.; ten Brinke, G.; Ikkala, O. *Adv. Mater.* **2001**, *13*, 117–121.

Fabrication of Nanomembranes/Nanotemplates. PS-PVP and HABA (1 mol of HABA:1 mol of 4-vinylpyridine monomer unit) were dissolved separately. PS-PVP solution was then added drop-by-drop to HABA solution, while the solution was heated close to the boiling point of the solvent in an ultrasonic bath. The heating was very important for the reproducible formation of SMA. The resulting solution (the range of the total concentration PS-PVP + HABA from 0.1 to 3 wt %, the fraction of HABA 17.8 wt %) was kept overnight to complete hydrogen bonding. Thin films were prepared by dip-coating from the filtered solutions. Dip-coating was performed with the rates ranging from 0.1 to 1.0 mm s⁻¹. Nanomembranes were fabricated by selective extraction of HABA with methanol.

The PS-PVP copolymer exhibits spherical morphology in bulk when the structure is formed by a PVP core surrounded by a PS shell.²³ From SAXS experiments, we have found that the PS-PVP-HABA equimolecular assembly produces the hexagonal cylindrical bulk structure with a characteristic period of 23 nm.

Characterization of the Ordered Thin Films. The thickness of the polymer films was measured by an SE400 ellipsometer (SENTECH Instruments GmbH, Germany) with a 632.8 nm laser at a 70° incident angle. The pore fraction of the thin polymer films was estimated from the effective refractive index (n , measured with ellipsometry) using the following equation:²⁴

$$n^2 = \sum_i v_i n_i^2$$

where n_i and v_i are the refractive indices and volume fractions of the constituent phases of the thin film.

UV-vis spectra were recorded with a Cary 100 Scan UV-vis spectrophotometer (Varian, Inc.). Infrared spectra were recorded with a Bruker IFS 66v FTIR spectrometer in the transmission mode.

AFM imaging was performed by a Dimension 3100 (Digital Instruments, Inc., Santa Barbara, CA) scanning force microscope and a CP (Park Scientific Instrument, Inc.) in the tapping mode. The tip characteristics are as follows: spring constant 1.5–3.7 N m⁻¹, resonant frequency 45/65 Hz, tip radius about 10 nm. Analysis of AFM images (Fast Fourier Transform, center map) was performed with the WSxM software (Nanotec Electronica). Center-center distance histograms were built using center map collecting for at least 3000 centers of C₁.

Templating of Nanomembranes. Nickel was introduced into the cylindrical channels of the membrane via electrodeposition in the galvanostatic mode for 1000 s at 300 μA cm⁻² current density using Autolab/PGSTAT30 with the Watts bath, an Ag/AgCl reference electrode, and a platinum wire counter electrode.

Results

In the first step, SMA polymer films on Si-wafers were prepared by dip-coating. Under an optical microscope, the polymer films with thicknesses ranging from 20 to 100 nm (ellipsometry) are macroscopically and microscopically smooth and show no signs of HABA phase separation, such as crystals or stains. This suggests that HABA molecules are associated with PVP blocks building comblike polymer chains. The AFM scratch test gives the same film thickness as ellipsometry if the SMA film is modeled as a layer with an apparent refractive index of $n = 1.63$. Such an elevated value of the apparent refractive index as compared to that for PS-PVP (1.59) is attributed to the significant fraction of HABA.

FTIR spectroscopy provides evidence for the formation of hydrogen bonds between HABA and pyridine fragments of PVP detected from the shifts (δ) of PVP characteristic bands sensitive

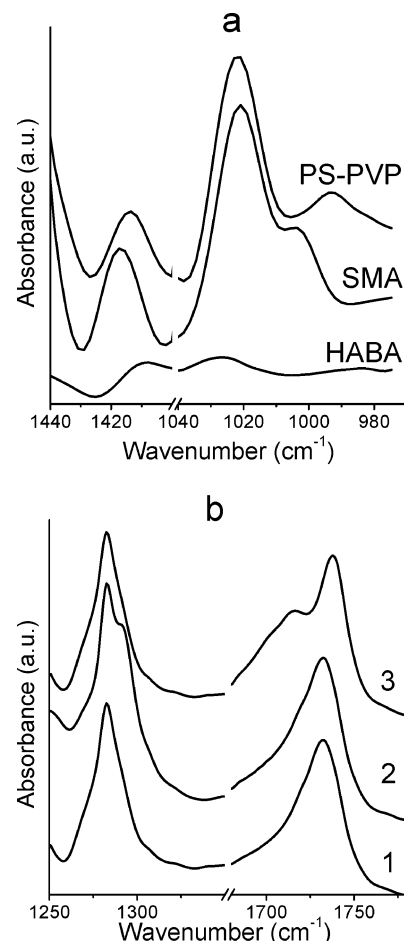


Figure 2. Infrared spectra of (a) PS-PVP, HABA, and SMA films, respectively, in the region of pyridine ring bands; (b) a model system HABA + pyridine in 1,4-dioxane (3) and in chloroform (2) in the regions of phenolic and carbonyl bands as compared to HABA without pyridine (1).

to the formation of hydrogen bonds at 1415 cm⁻¹ ($\delta = 5$ cm⁻¹) and 993 cm⁻¹ ($\delta = 8$ cm⁻¹) as compared to PS-PVP spectra (Figure 2a).²⁵ This result is very similar to those reported elsewhere for hydrogen bonds of PVP with PDP.^{25,26} To improve our understanding for the mechanism of the interaction between PVP blocks and HABA in different media, we study interactions in the model system consisting of HABA and pyridine in 1,4-dioxane and chloroform solutions (Figure 2b, lines 2 and 3). As a reference, we use the FTIR spectra of HABA in 1,4-dioxane (Figure 2b, line 1). We found a very pronounced difference between the spectra in 1,4-dioxane and chloroform. Hydrogen bonding involving carbonyl groups results in the appearance of a new band at 1720 cm⁻¹ in 1,4-dioxane, while a new band at 1275 cm⁻¹ in chloroform indicates the formation of hydrogen bonds with phenolic groups of HABA. Consequently, the spectra give evidence of switching between different mechanisms of hydrogen bond formation in different solvents, which is introduced by the competition with solvent.

Important information for the understanding of the SMA film structure was extracted from the analysis of UV-vis spectra. HABA demonstrates the very intensive absorption peak at 382.0 nm (Figure 3a). In contrast, the SMA film spectrum shows a

(23) Ruokolainen, J.; Saariaho, M.; Ikkala, O.; ten Brinke, G.; Thomas, E. L.; Torkkeli, M.; Serimaa, R. *Macromolecules* **1999**, *32*, 1152–1158.

(24) Wedgewood, A. R.; Seferis, J. C. *Polym. Eng. Sci.* **1984**, *24*, 328.

(25) Lee, J. Y.; Painter, P. C.; Coleman, M. M. *Macromolecules* **1988**, *21*, 954–960.

(26) Ruokolainen, J.; ten Brinke, G.; Ikkala, O.; Torkkeli, M.; Serimaa, R. *Macromolecules* **1996**, *29*, 3409–3415.

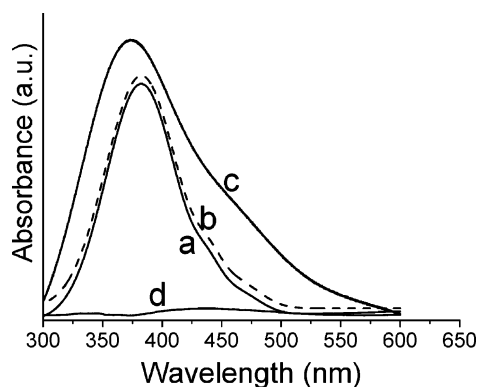


Figure 3. UV-vis spectra of (a) HABA 1.8×10^{-3} g L $^{-1}$ chloroform solution, 10 mm quartz cell, (b) SMA 0.01 g L $^{-1}$ chloroform solution, 10 mm quartz cell, (c) the SMA 110 nm thick film, and (d) the SMA nanotemplate after HABA extraction.

blue shift of the main peak (367.4 nm) as compared to the spectra of HABA or SMA solutions (Figure 3a–c). It is a strong argument for H-aggregation of HABA (parallel face-to-face, according to the molecular exciton model).^{27,28} This specific structure may play an important role in the morphology of the film.

The detailed investigation of SMA films with AFM shows the dependence of the morphology on the deposition conditions. SMA films deposited from chloroform solution demonstrate the terrace formation (Figure 4a). The films are very smooth inside of the terraces with a rms roughness of about 0.3 nm for a $1 \times 1 \mu\text{m}^2$ lateral scale. In contrast, SMA films deposited from 1,4-dioxane are flat and featureless. The rms roughness is 0.15 nm as measured on a $1 \times 1 \mu\text{m}^2$ lateral scale. We did not visualize a fine structure of the materials because of the poor contrast between the mechanical behavior of PS and PVP + HABA domains in the film.

In the second step, the films were rinsed in methanol (selective solvent for PVP and HABA) for 2 min. We expected that methanol destroys supramolecular assemblies and removes selectively HABA from SMA, leaving cylindrical cavities in the film. We used the absorption peak at 382.0 nm in UV-vis spectra to examine the films after the rinsing procedure. Comparing the band intensities for the polymer film before (Figure 3c) and after (Figure 3d) the rinsing, we may conclude that HABA was completely washed out with methanol from the film.

The AFM scratch test showed no significant difference in film thickness before and after washing. It gives evidence that almost all HABA is located in PVP domains because the thickness of the PS matrix remains almost unchanged. Ellipsometric data for the same film thickness were fitted with the apparent refractive index $n = 1.50 \pm 0.01$. Such a decrease of n from 1.63 for SMA film (before washing) to 1.5 (after washing) is effected by the formation of porous morphology of the film due to the elimination of HABA. Note that the obtained n value is much lower than $n = 1.59$ for the PS-PVP reference film, which gives additional evidence for the formation of a membrane with porous morphology. The estimated volume fraction of the pores in the membrane ($n_{\text{PS}} = n_{\text{PVP}} = 1.59$) is in good agreement with the concentration of HABA in the initial mixture (17.8%).

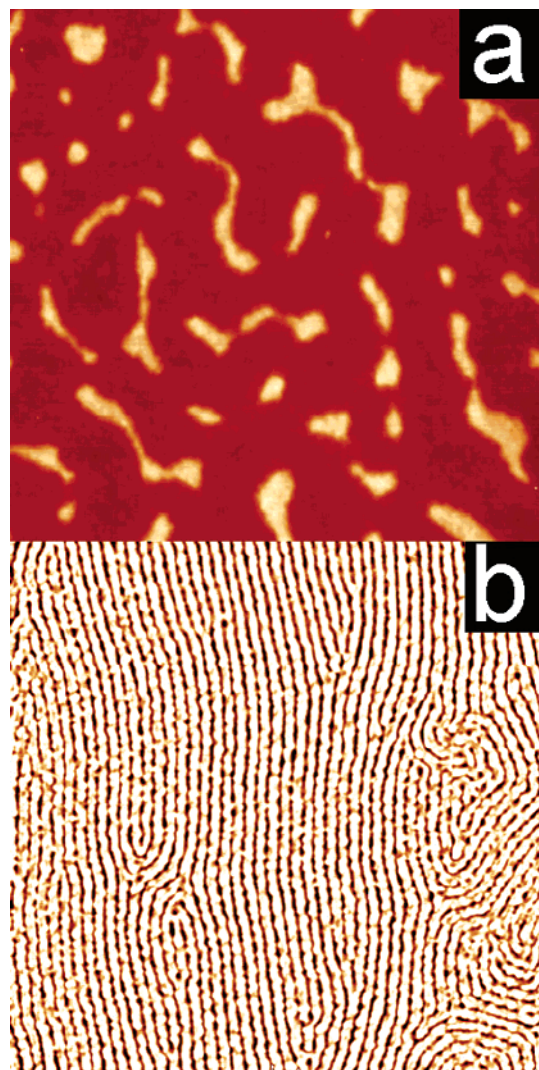


Figure 4. AFM images of SMA films (a) dip-coated from chloroform solution, 40 nm thick, lateral scale $16 \times 16 \mu\text{m}^2$, z scale 30 nm, and (b) dip-coated from chloroform solution and washed with methanol, 40 nm thick, lateral scale $1 \times 1 \mu\text{m}^2$, z scale 5 nm.

Rinsing with methanol develops the fine structure of the films clearly observed with AFM. The film deposited from chloroform shows well-aligned stripes (Figure 4b) which can be assigned as CII cylindrical domains.¹⁰

The film deposited from 1,4-dioxane and washed with methanol demonstrates caves of about 8 nm in diameter which are a projection of C \perp domains (channels) with a periodicity of about 24 nm (Figure 5a). The center-center distance analysis reveals a relatively narrow distribution of spacing between channels with a standard deviation <20% as visualized by the Gaussian fit (Figure 5b) and Fourier transform image (inset). The center-center distance distribution found for the membranes prepared from the “as-deposited” films is comparable to the distribution of an optimized PS-PVP film obtained by the “neutral surface” approach.²⁹ We observed the same level of order for different film thicknesses ranging from 20 to 100 nm.

Alignment of cylindrical domains in SMA films can be easily changed with the appropriate solvent. For example, this was observed after the 60 nm thick film deposited from 1,4-dioxane

(27) McRae, E. G.; Kasha, M. *J. Chem. Phys.* **1958**, *28*, 721–722.

(28) Dante, S.; Advincula, R.; Frank, C. W.; Stroeve, P. *Langmuir* **1999**, *15*, 193–201.

(29) Guarini, K. W.; Black, C. T.; Yeung, S. H. I. *Adv. Mater.* **2002**, *14*, 1290–1294.

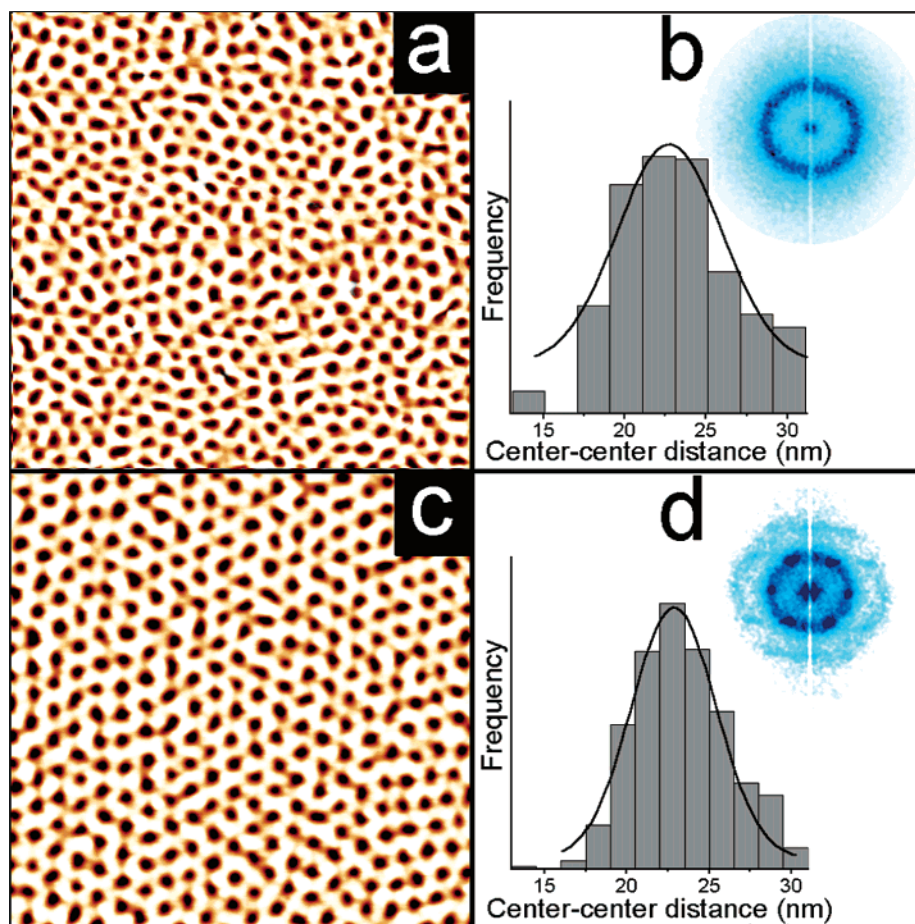


Figure 5. AFM images of SMA films: (a) dip-coated from 1,4-dioxane solution, dried, and washed with methanol, 40 nm thick, lateral scale $500 \times 500 \text{ nm}^2$, z scale 5 nm, (b) histogram of center–center distances with Gaussian fit and FFT image of (a), (c) SMA after being swelled in 1,4-dioxane vapor, dried, and washed with methanol, 40 nm thick, lateral scale $500 \times 500 \text{ nm}^2$, z scale 5 nm, (d) histogram of center–center distances with Gaussian fit and FFT image of (c).

($C\perp$ pattern, Figure 5a) was annealed in a saturated vapor of chloroform for 30 min at room temperature. Once the sample was removed from the chamber, it dried in about 1 s. We then rinsed it with methanol. The film reveals the characteristic $C\parallel$ morphology similar to the morphology obtained directly after deposition from chloroform solution. Oppositely, SMA films deposited from chloroform with $C\parallel$ alignment were reoriented into hexagonal $C\perp$ morphology after being annealed in a 1,4-dioxane saturated vapor atmosphere for 30 min at room temperature. Moreover, swelling of the SMA film in 1,4-dioxane vapor results in a significant increase of order (Figure 5c). The center–center distance distribution is very narrow (standard deviation 9%, Figure 5d). Six sharp first order peaks and the presence of higher order reflections are clearly seen on the FFT image (Figure 5d, inset), demonstrating the almost perfect hexagonal order spreading over the area of $0.2/2 \mu\text{m}^2$. We assume that the well-ordered structure is promoted by aggregation of HABA molecules. The re-alignment occurring in SMA is reversible, relatively fast, and can be repeated several times for films that are not rinsed.

The kinetics of the re-alignment was monitored by analyzing the morphology of the films as a function of time and swelling degree (evaluated with ellipsometry). We found out that the re-alignment began upon exposure to a saturated vapor of solvent if the swelling approached a 2.5 times increase in the film thickness (in our experiments, this swelling degree was observed

in 10 min). The completed re-alignment was then approached in about 10 min. Very similar kinetics was observed for different solvents.

It is noteworthy that the same behavior was found for substrates of different chemical compositions, for example, PS brush, gold, ITO-glass, and Ni. Thus, the film morphology is insensitive to the substrate surface nature.

The fast switching between two different alignments of the cylindrical domains and the indifference of alignment to the substrate surface energy provide evidence for the very strong modification of the SMA film behavior as compared to that of BC films. Reconstruction of BC film morphology by vapor or thermal annealing was reported in the literature.^{10,11,19} However, this process is typically very slow and usually results in morphologies representing the coexistence of different alignments of nanodomains. Perpendicular orientation/reorientation requires a combination of thermal annealing and a strong electric field and occurs even more slowly than the above process.^{14,30} The “neutral surface” approach is limited by a film thickness of about one period and requires sufficient time and temperature.²⁹ In contrast, the SMA films demonstrate ordering in either $C\perp$ or $C\parallel$ orientation without influence of additional external stimuli.

(30) Böker, A.; Knoll, A.; Elbs, H.; Abetz, V.; Müller, A. H. E.; Krausch, G. *Macromolecules* **2002**, *35*, 1319–1325.

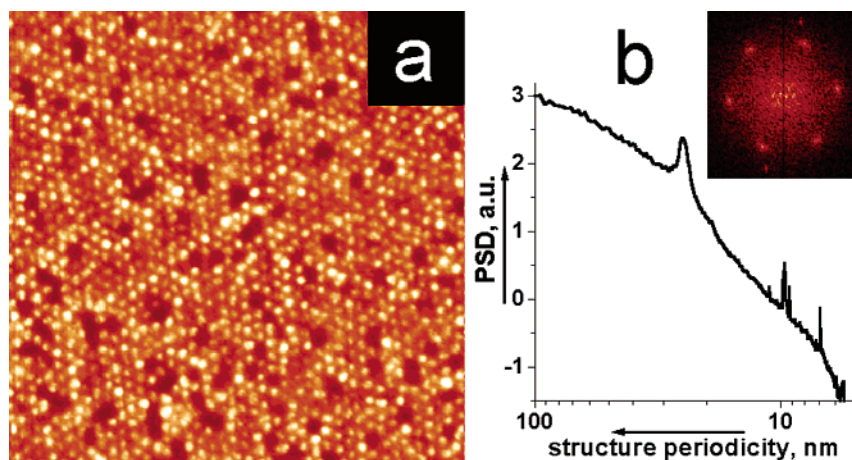


Figure 6. Ni dots electrodeposited throughout 45 nm thick PS-PVP nanotemplate, lateral scale $1 \times 1 \mu\text{m}^2$: (a) topography image, z scale 30 nm, (b) power spectrum density, the main peak (24 nm) corresponds to the SMA periodicity (inset, FFT image of (a) showing perfect hexagonal ordering of Ni dots). Occasional lacunas appear due to the inhomogeneity of electrodeposition.

The experiments were performed in different solvents, and we found that the stability of the $C\perp$ alignment increased with the increased reactivity of the solvent in the formation of hydrogen bonds. For example, the $C\parallel$ alignment was found in toluene and chloroform. The SMA film deposited from THF exhibits a coexistence of $C\parallel$ and $C\perp$ structures, while in 1,4-dioxane the $C\perp$ structure is stable.

Taking into account the above-mentioned behavior and the structure of the SMA film, we may speculate that the reversible and dynamic supramolecular aggregation between PVP and HABA via hydrogen bonds may introduce the mechanism of self-adaption of the interface composition. Redistribution of HABA molecules between bulk and interface occurs so that a minimum interface energy may be approached for the particular alignment and environment, making the morphology insensitive to the confining surface. Solvent plays a very important role competing with PVP for HABA molecules so that a subtle interplay between HABA–PVP–solvent interface interactions may result in conditions switching in the mechanism, as is proven by the FTIR spectra (Figure 2b). This mechanism helps one to overcome surface-dominant alignment as compared to BC films. The detailed investigation of the mechanism requires consideration of many parameters, and it is out of the focus of this paper. The prevalent role of HABA is the subject of our future investigations.

It is noteworthy that the walls of the channels formed after rinsing with methanol are constituted from the brush of PVP chains. The free space left by HABA molecules can be reversibly occupied by swollen PVP chains upon exposure of the membrane to selective solvent or acidic aqueous solution. Thus, the fabricated membranes belong to the class of smart membranes with uniform reactive channels of a narrow distribution in size.

In the third step, the nanomembrane prepared by rinsing in methanol the SMA film in the $C\perp$ orientation on the gold coated Si-substrate was filled with Ni clusters. Nickel was introduced into the cylindrical channels of the membrane via the electrodeposition method. We then washed out the polymer template with THF. The well-ordered lattice of Ni dots 15–20 nm in the diameter, 10 nm in height, and with a 24 nm period was observed with AFM (Figure 6). Taking into account the

widening effect of the AFM tip,³¹ we found that the apparent size of the dots is in good agreement with the nanotemplate channel diameter (8 nm). Few defects (lacunas) appear in the array of Ni dots due to the nonuniform electrodeposition kinetics of the metal clusters in nanochannels. Besides the potential application, this experiment gives evidence that the cylindrical channels cross the membrane from the top to the bottom.

Summary

We report on our finding of the unexpected behavior of the supramolecular assembly of a PS-PVP block copolymer with HABA molecules resulting in the $C\perp$ alignment of cylindrical nanodomains. The alignment is insensitive to the composition of the confined surface. The film can be reversibly switched from the perpendicular to parallel orientation and vice versa upon exposure to 1,4-dioxane and chloroform vapor, respectively. The re-alignment in different solvents is a relatively fast (tens of minutes) process. The perpendicular orientation of the cylinders can be approached without applying strong external stimuli (e.g., electrical field), which is in contradiction to the surface reconstruction effect usually observed for BC thin films.

We explain the observed behavior by the specific intermolecular aggregation of HABA molecules which can overcome the confining surface dominated reconstruction and stabilize the perpendicular alignment in 1,4-dioxane due to the self-adaptive behavior of SMA surface. HABA molecules can be selectively and completely extracted from the ordered films, resulting in membranes with an ordered lattice of cylindrical nanochannels. The walls of the nanochannels are formed by the reactive PVP brush.

We demonstrate that the channels can be filled with metal, for example, nickel, by electrochemical deposition to fabricate an array of ordered nanodots or nanowires.

Acknowledgment. BMBF (grant 05KS1BPA/4) is gratefully acknowledged for financial support. S.M. acknowledges the support of the Center for Advanced Materials Processing, Clarkson University.

JA036085W

(31) Vesenka, J.; Manne, S.; Giberson, R.; Marsh, T.; Henderson, E. *Biophys. J.* **1993**, *65*, 992–997.